

APPLICATION OF THE CFS PML TO THE FDTD SOLUTION OF WAVE-STRUCTURE INTERACTION PROBLEMS

J.-P. BERENGER

Centre d'Analyse de Défense
16 bis, Avenue Prieur de la Côte d'Or 94114 Arcueil, France
berenger@cad.etca.fr

I - INTRODUCTION

As solving wave-structure interaction problems with the FDTD method, the perfectly matched layer (PML) absorbing boundary condition (ABC) can be set quite close to the structure of interest [1], so that the overall computational domain is widely reduced in comparison with previously used ABC's. Nevertheless, the PML must be some cells in thickness and it typically consumes 20-50 % of the overall computational time. It would be desirable if this thickness were reduced. From theoretical investigations in [2], the complex frequency shifted (CFS) PML [3] is a candidate in view of achieving such an objective. This is illustrated in the present paper by means of numerical experiments with three-dimensional structures.

II - THE CFS PML

In the CFS PML, the stretching coefficient of the normal PML is replaced by

$$s_x = \kappa_x + \frac{\sigma_x}{\alpha_x + j\omega\epsilon}, \quad (1)$$

where α_x is homogeneous to a conductivity and κ_x is real. An effective FDTD discretization has been proposed in [4] and the features of the numerical reflection from this PML have been discussed in [2]. From (1), frequency

$$f_\alpha = \frac{\alpha_x}{2\pi\epsilon} \quad (2)$$

is a key parameter. For $f \gg f_\alpha$ the CFS PML acts as a normal PML. Conversely, for $f \ll f_\alpha$ coefficient (2) is real so that the CFS PML only acts as a real stretch of coordinates ($\kappa_x + \sigma_x / \alpha_x$). From this, for $f \ll f_\alpha$ traveling waves are not absorbed, but evanescent waves can be annihilated by the real stretch.

III - WAVE-STRUCTURE INTERACTIONS

Schematically, the field surrounding a PEC structure struck by an incident wave is composed of evanescent fields, below the resonance frequency, and traveling waves, above the resonance frequency. By assuming that the evanescent fields decrease to a small value upon a distance of the order of the largest size of the structure w , one can arrive to the following optimum parameter α_x [2]

$$\alpha_0 = \frac{\epsilon c}{w} \quad (3)$$

Then, the absorption of low frequency evanescent fields is about equal to the absorption of traveling waves [2]. This allows a reasonable absorption of evanescent fields to be achieved, resulting in a small numerical reflection of these fields. Moreover, (2) and (3) yield $f_\alpha(\alpha_0) = f_0 / \pi$, where f_0 is the resonance frequency $c/2w$, so that the transition between the two regimes of the CFS PML is about the transition between evanescent and traveling waves surrounding the structure. From this, all the surrounding waves are absorbed by the CFS PML with sufficient and not too strong absorption [2].

IV - NUMERICAL EXPERIMENTS

As in two dimensions [2], three-dimensional experiments with CFS PMLs easily show that the best results are obtained with α_x in the range $\alpha_0 / 2$ to $2 \alpha_0$. All the results shown in this paper were computed with $\alpha_x = \alpha_0$, and PMLs - either normal or CFS - set only two FDTD cells from the scattering structure.

Fig. 1 shows the E field at two points on the surface of a 500 cells thin plate struck by a unit-step incident wave [5], for 4, 6, 8, 12 cells thick CFS PMLs. The conductivity is quadratic and $R(0) = -40$ dB. As observed, the numerical reflection is small with a 4-cell CFS PML, and negligible with an 8-cell one. Fig. 2 shows similar experiments with the 126*237*60-cell airplane in [5].

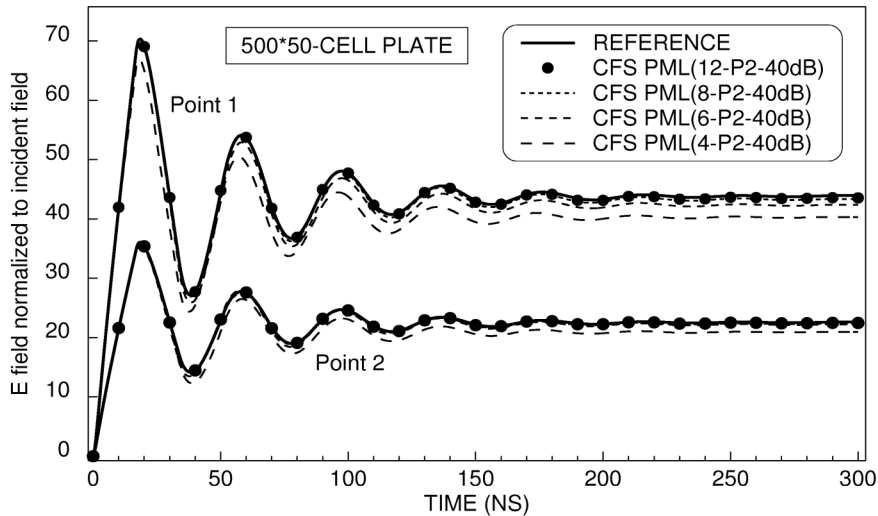


Fig. 1 - E field at two locations on a 500*50*0-cell thin plate ($\Delta x = \Delta y = \Delta z = 1$ cm) computed with 4, 6, 8, and 12 cells thick CFS PMLs ($\alpha_x = \alpha_0$).

Fig. 3 compares the 500-cell plate results obtained using the 6-cell CFS PML, with results in paper [5] that describes an easy implementation of optimum normal PMLs in three-dimensional computer codes. Two PMLs are compared with the CFS PML, a 10-cell normal PML [5], and a 9-cell normal PML with some refinements (the so-called A interface and a slight real stretch of coordinates, see [5]). As observed, the 6-cell CFS PML yields results at least as

good as those of the 10-cell and 9-cell normal PMLs. Fig. 4 shows a similar comparison for the airplane. For this structure, the 4-cell CFS PML yields results as good as the 7-cell or 5-cell normal PMLs.

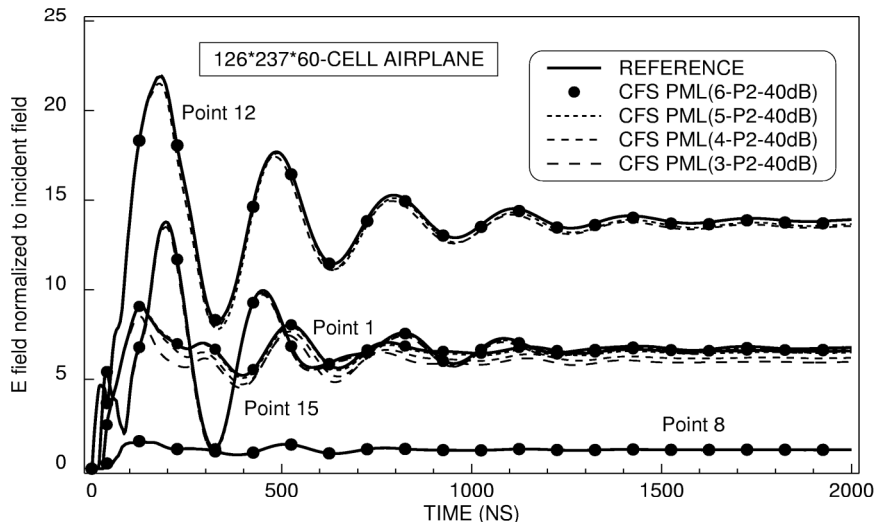


Fig. 2 - E field at four locations on a 126-237-60-cell airplane ($\Delta x = 25$ cm, $\Delta y = \Delta z = 16.66$ cm) computed with 3, 4, 5, and 6 cells thick CFS PMLs ($\alpha_x = \alpha_0$).

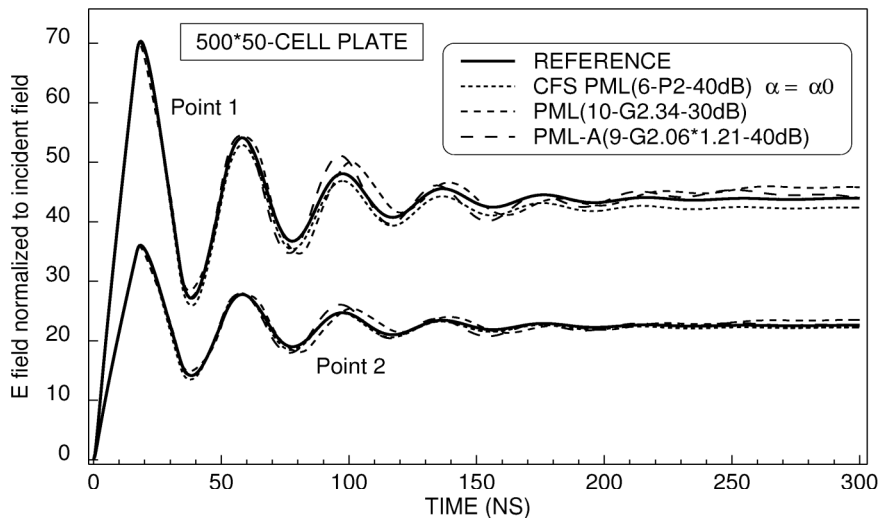


Fig. 3 - Comparison of results computed using the 6 cells thick CFS PML with optimized PML and PML-A in [5], for the 500-50-0-cell plate.

The observations in the above figures can be reproduced with other structures and other time-domain forms of the incident wave. With (3), the CFS PML that allows a given level of accuracy to be obtained (acceptable results as in Figs. 3 and 4, or perfect results superimposed to the reference) is thinner than the normal PML, even when this last one is optimized by the method in [5]. Notice that the advantage of the CFS PML grows with the duration of the calculation since the thickness of normal PMLs grows with this parameter [1], [5].

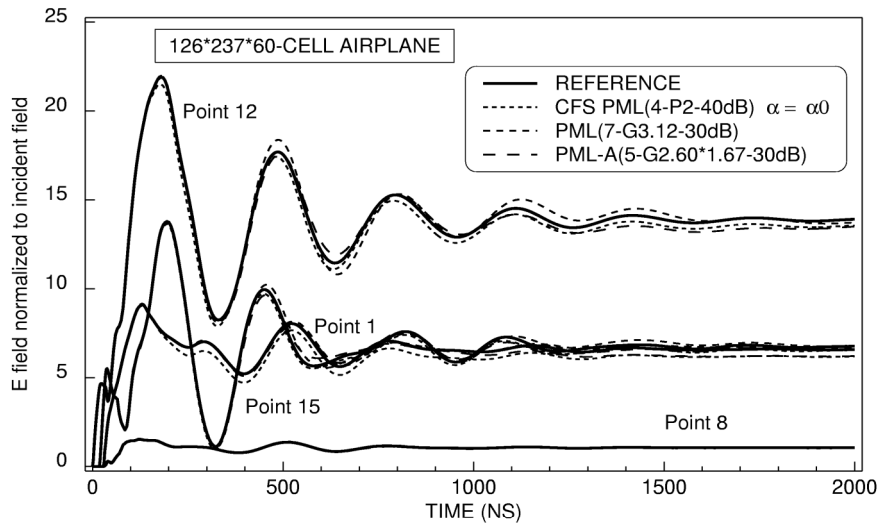


Fig. 4 - Comparison of results computed using the 4 cells thick CFS PML with optimized PML and PML-A in [5], for the 126-237-60-cell airplane.

V - CONCLUSION

By an adequate choice of parameter α_x , the CFS PML allows the PML thickness to be reduced in comparison with normal PMLs. Moreover, since it has been recently introduced, some progress can be hoped for. Especially, it would be desirable if the critical parameters that impact the accuracy were found, so as to be able to design the PML in function of the structure of interest, as can be done with normal PMLs [1], [5].

From a practical point of view, significant reductions of computational requirements can be expected, probably in the range 10-25 % in comparison with optimized normal PMLs [5]. Nevertheless, further investigations are needed so as to render the use of the CFS PML as easy and reliable in applications as normal PMLs with implementation [5].

REFERENCES

- [1] J.-P. Bérenger "Perfectly matched layer for the FDTD solution of wave-structure interaction problems" *IEEE Trans. Ant. and Propag.*, vol. 44, no. 1, pp. 110-117, 1996.
- [2] J.-P. Bérenger "Numerical reflection from FDTD-PML's : A comparison of the split PML with the unsplit and CFS PML's" *IEEE Trans. Ant. and Propag.*, vol. 47, no. 10, pp. 258-265, 2002.
- [3] M. Kuzuoglu and R. Mittra "Frequency dependence of the constitutive parameters of causal perfectly matched absorbers" *IEEE Micr. And Guid. Wave Let.*, vol. 6, no. 12, pp. 447-449, 1996.
- [4] J. A. Roden and S. D. Gedney "An efficient FDTD implementation of the PML with CFS in general media" *Proc. IEEE Antennas and Propagat. Soc. Int. Symposium*, Salt Lake City, USA, Vol. 3, pp. 1362-1365, July 2000.
- [5] J.-P. Bérenger "Making use of the PML absorbing boundary condition in coupling and scattering FDTD computer codes" *IEEE Trans. Elec. Compat.*, submitted, 2002.